*International Journal of Research in Advent Technology, Vol.6, No.8, August 2018*
*E-ISSN: 2321-9637*
*Available online at www.ijrat.org*

# Investigation on infrared reflective property of Mg-doped bismuth titanate for the application of cool home coating

P.Meenakshi [1], M.Pavithra [2], A.K.N.Pavithra [3], M.Selvaraj [4]
*Corrosion and Materials Protection Division [1,2,3,4], CSIR-Central Electrochemical Research Institute, Karaikudi, 630003.[1,2,3,4]*
*Email: meenachrist76@gmail.com[1] , selvaraj58@gmail.com[4]*

**Abstract-** This paper deals with a synthesis of magnesium doped bismuth titanate (Mg-BTO) at various doping concentrations (0.25M, 0.50M and 0.75M) for the application of infrared reflective pigment. The infrared (IR) reflectance property of synthesized Mg-BTO was studied using UV-Vis-NIR diffuse reflectance spectrophotometer. The synthesized Mg-BTO shows an IR reflectance value of about ~R=99%. The crystalline nature, structural property, morphology were analyzed using X-ray diffraction technique (XRD), Scanning electron microscopy (SEM), Transmission electron microscopy (TEM). Apart from IR reflectance study, the thermal study and the stability test were also performed to confirm the usage of synthesized Mg-BTO pigment as IR reflective pigment. The consolidated results shown by synthesized Mg-BTO confirm its application as infrared reflective pigment for the cool home coating to minimize the energy usage.

**Index Terms-** Magnesium doped bismuth titanate; pyrochlore structure; Infrared reflectance.

## 1. INTRODUCTION

Solar light consists of spectrum of radiation which includes 42% of visible radiation [1-2], 5% of ultraviolet radiation and 53% of infrared radiation [3-5]. Among this solar radiation spectrum, infrared (IR) radiation is responsible for the production of heat in the earth's atmosphere. These IR radiations are absorbed by the objects and become hot, which is responsible for the heat generations. Rising of energy cost, pronounces urban heat-island effect and global warming increases the need for intelligent solar heat management solution like infrared reflective pigments. The roof of the building in the urban area absorbs maximum amount of infrared radiation and conduct the heat into the building. These hot buildings radiate the heat and warm the air in the surroundings. In many countries, around 40% of the energy usage is being done by the buildings. Due to this reason a building with an infrared reflective outdoor coating will decrease the energy usage.

Bismuth titanate belongs to a large family including various phases of Bi-O-Ti system. Bismuth titanate ($Bi_4Ti_3O_{12}$) has perovskite structure of $ABO_3$ form while the $Bi_2Ti_2O_7$ has a pyrochlore structure [6]. Synthesis of pyrochlore structure of bismuth titanate is a challenging task due to its thermal instability at a temperature of above 650º C. On calcination at higher temperature, $Bi_2Ti_2O_7$ will be decomposed to $Bi_4Ti_3O_{12}$ and $Bi_2Ti_4O_{11}$ [7]. The condition for the pyrochlore structure to get stable is that the size factor ratio limit should be in the range of $1.46 < r(A^{3+})/r(B^{4+}) < 1.80$ [8]. But the size factor ratio value for $Bi_2Ti_2O_7$ is 1.93 [9], which exceed the limit to become an unstable structure. Bismuth based pyrochlore structure have been widely studied for its dielectric properties [10-16] and photocatalytic application [17-20].

In recent days a large number of IR reflective pigments were reported. But the current scenario of the pigment industry is the development of IR reflective pigment with the properties of non-toxic and cheaper in cost to help in the energy savings [21].

Many NIR reflective pigments like Fe-doped $MgTiO_3$ [22], bismuth titanate [23]. chromium doped alumina [24] and Mn-doped $ZnAl_2O_4$ [25], ultramarine pigment [26] with NIR reflectance of 74%, 95%, 70.5%, 50.55% and 65% in different color shades and good IR reflectance values were reported. In current scenario a cool pigment with high NIR reflectance, cheaper in cost and less toxic is more needed.

Recently we have reported a bismuth titanate as an infrared reflective pigment with an IR reflectance value of ~95% [23]. In this paper we have doped magnesium in the bismuth titanate lattice to enhance its reflectance value and its thermal stability. Magnesium ion is a suggested A-site dopant in previous literatures [27] to replace the bismuth (Bi) ions and additionally magnesium has good emissivity value of 0.55 than the bismuth (0.34). The Mg-BTO shows better IR reflectance value and thermal stability than the undoped bismuth titanate (BTO).

## 2. EXPERIMENTAL SECTION

### 2.1. *Materials required*

The chemicals bismuth nitrate (Merck), Butyl titanate (Acros Organics), Magnesium nitrate (sigma Aldrich), Nitric acid (Merck), Ammonium hydroxide (Rankem) and Sodium hydroxide (Fischer Scientific) used for synthesis are analytical grade and used without further purification.

### 2.2. *Synthesis of magnesium doped bismuth titanate*

A stoichiometric amount of bismuth nitrate and magnesium nitrate were dissolved in an acidic solution. The butyl titanate solution was treated with aqueous ammonium hydroxide to form a white precipitate. Then the nitric acid solution is added to dissolve the white precipitate. After a complete dissolution of bismuth nitrate and magnesium nitrate, the titanate solution was added. The reaction solution was allowed to stir under constant stirring and heated on a hot plate for 1 hour. Then the sodium hydroxide solution was added drop wise till the precipitation occurs. Then the precipitate was transferred to the Teflon lined stainless steel autoclave and heated to the temperature of 180 ºC. The resulting powder was washed repeatedly using distilled water and the powder was dried in an oven for 24 h at 80 ºC. The dried powder was ground using a mortar and pestle before further calcination and characterization.

### 2.3. *Characterization Techniques*

The purity and the phase analysis of the samples were performed by powder X-ray diffraction using a Ni-filtered Cu $K_\alpha$ radiation with a powder X-ray diffraction (XRD) (Bruker). Data were collected by a step-scanning from 2θ angle of 10º - 80º. The surface morphology was analysed using the scanning electron microscope (SEM) (HITACHI, S-3000H) and the SAED pattern was also analysed using Transmission Electron Microscope (TEM) ( FEI, The Netherlands) ( Tecnai 20 G2 (FEI make). The TEM samples were well dispersed in ethanol solution using ultrasonicator; drop cast on the copper grid and dried. The NIR reflectance of the pigments and pigment coated steel substrate were measured using UV-Vis-NIR Spectrophotometer (VARIAN CARY 500 Scan) with an integrating sphere attachment using poly-tetrafluoroethylene (PTFE) as a reference at a wavelength range of 200 nm to 2500 nm. The NIR solar reflectance (R*) in the wave-length range from 700 to 2500 nm was calculated in accordance with the ASTM standard number G173-03 as described elsewhere [19]. Then, the NIR solar reflectance or the fraction of solar radiation incident at wavelengths between 700 and 2500 nm that is reflected by a surface is the irradiance-weighted average of its spectral reflectance, r(λ) can be determined that is

$$R* = \frac{\int_{700}^{2500} \boldsymbol{r(\lambda) i(\lambda) d(\lambda)}}{\int_{700}^{2500} \boldsymbol{i(\lambda) d(\lambda)}}$$

Where r (λ) is the spectral reflectance ($Wm^{-2}$) obtained from the experiment and i(λ) is the solar spectral irradiance ($Wm^{-2}$ $nm^{-1}$) obtained from ASTM standard G173-03. The color of the pigment was measured based on The Commission Internationale del' Eclairage (CIE) through L*a*b* 1976 color scales (CIE-LAB 1976 color scales). In this method the L* denotes the lightness axis (L* = 0 for black and L* = 100 for white), a* denotes green (-)/ red (+) axis, b* denotes blue (-)/ (+) yellow axis. Te parameter C* (Chroma) denotes the saturation of the color and the hue angle ($h^o$) is expressed in degrees and ranges from 0º to 360º and can be calculated using the formula $h^o = \tan^{-1}(b^*/a^*)$.

## 3. RESULTS AND DISCUSSIONS

### 3.1. X-ray Diffraction studies

Fig.1. shows the XRD pattern of Mg-doped bismuth titanate (Mg-BTO) at various concentrations. The Mg-BTO shows a pyrochlore phase ($Bi_2Ti_2O_7$) of bismuth titanate. The stability of the pyrochlore structure is determined by the size factor ratio of the ions occupying positions A and B. The limit of size factor ratio for pyrochlore structure is $1.46 < r(A^{3+})/r(B^{4+}) < 1.80$. The size ratio for $Bi_2Ti_2O_7$, $r(Bi^{3+})/ r(Ti^{4+})$ is 1.93 (exceeds the limit range) [28]. So the $Bi_2Ti_2O_7$ phase is not stable, which decomposes into $Bi_4Ti_3O_{12}$ and $Bi_2Ti_4O_{11}$ above 612 ºC. Since the thermal stability of the pyrochlore structure can be enhance by inserting a metal cations with an ionic radius smaller than bismuth ($Bi^{3+}$=1.14Å) at the bismuth position which reduces the total ionic radius of the atoms in sublattice A. The diffraction study was carried out based on different concentrations of dopants. Bismuth titanate doped with 0.25M, 0.50M, 0.75M Mg in bismuth site results in $Bi_2Ti_2O_7$ phase (pyrochlore). The pyrochlore structure ($Bi_{2-x}Mg_xTi_2O_7$, x=0.25M,0.50M, 0.75M) had a size ratio values of 1.79, 1.76, 1.73. The reduction in size ratio value is due to the insertion of metal cation with smaller ionic radii than the bismuth ions in the bismuth position. This shows that by doping higher concentration of magnesium ions results in pyrochlore structure due to generation of better conditions for spatial arrangement of the atoms in the pyrochlore structure. XRD peaks of $Bi_{2x}Mg_xTi_2O_7$ (x= 0.25, 0.50, 0.75) compound were well matched with the standard JCPDS [00-032-0118] which conforms the formation of $Bi_2Ti_2O_7$ phase (pyrochlore structure). The peaks at 30.1º, 28.8º, 34.9º, 38.1º, 50.1º and 59.5º were formed due to the

formation of (444), (622), (800), (662), (880) and (1244) planes of pyrochlore bismuth titanate [29]. Peaks of other phases and peaks corresponding to $Bi_2O_3$, MgO and magnesium titanate were also not formed which confirm the purity of the product.

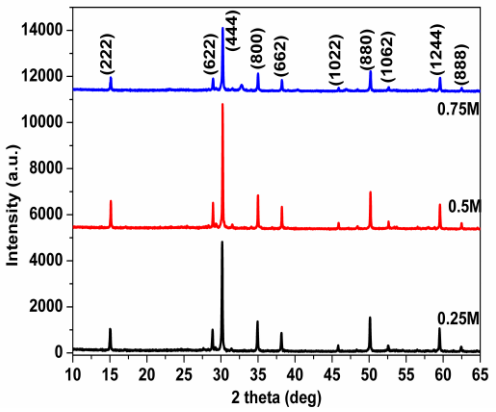


Fig.1. XRD pattern of Mg-doped bismuth titanate at various concentrations of Mg (0.25M, 0.50M and 0.75M)

### 3.2. *Band gap energy*

The absorbance graph of the Mg-BTO is shown in fig.2. The band gap energy was calculated using the formula, E=hc/λ. Where h= Planck's constant, c= velocity of light, λ= cut-off wavelength. The band gap of the compounds with 0.25M, 0.50M, and 0.75M doping are 2.90eV, 2.86eV and 2.79eV. These values are well matched with the reported value for pyrochlore $Bi_2Ti_2O_7$ structure [29, 30]. These values also confirm the formation of pyrochlore structure. With increase in the amount of doping, the density of states of these dopants increase and forms a continuum of states just like in the bands and effectively the band gap decreases.

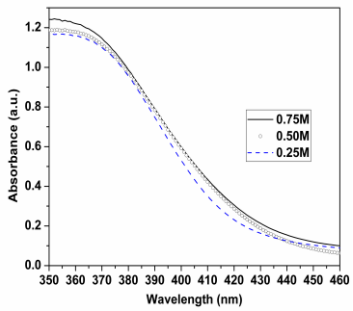


Fig.2. Absorbance graph of Mg-doped bismuth titanate

### 3.3. *Particle size analysis*

The mean particle size of the Mg-BTO is 0.305 µm, 0.316 µm and 0.412 µm for 0.75M, 0.50M and 0.25M Mg-BTO. The mean particle diameter of Mg-BTO is an average value of measured particle.

### 3.4. *Morphology study*

The morphology of the Mg-BTO was viewed through FESEM technique and the FESEM images of the same were shown in Fig.3. The particle size of Mg-BTO gets decreases on increasing the concentration of dopants. This is due to restriction of particle growth by the insertion of dopant ions in the lattice of bismuth ions.

### 3.5. *HRTEM Studies*

The HRTEM image of Mg-BTO is shown in fig 4a. The enlarged view of circled area of fig 4a is shown in fig 4b. The d-spacing value was calculated from the fringes seen in fig 4b. The d-spacing value of 0.215 nm was matched with d-spacing value of (444) plane of $Bi_2Ti_2O_7$ structure, which was well correlated with results of XRD technique for the formation of pyrochlore structure of $Bi_2Ti_2O_7$. The d-spacing value for (444) plane of pure $Bi_2Ti_2O_7$ is 0.298nm [29]. This result shows that the d-spacing value of Mg-BTO get decreases than the d-spacing value of pure $Bi_2Ti_2O_7$. This reduction of d-spacing value is due to the insertion of smaller ionic radii magnesium ions into the bismuth lattice. The crystalline nature of Mg-BTO was also confirmed from the SAED pattern which was shown in fig.4c.

### 3.6. *Chromatic properties*

The chromatic properties of the synthesized pigment have been evaluated using CIE 1976 color coordinate system and the values were summarized in table.1. The color coordinates parameters (L*, a*, b*) of Mg-BTO shows that the pigment in white color and has high lightness property. The photograph of Mg-BTO of various dopant concentrations is shown in fig.5. The L* value represents the lightness (brightness) of the pigment. The L* values of Mg-BTO tabulated below shows that the L* values get increases by increasing the dopant concentration. This shows that the synthesized pigment is in lighter shade color. In all cases of doping, the L* values are above the value of 95, which confirms the more brightness nature of the pigment.

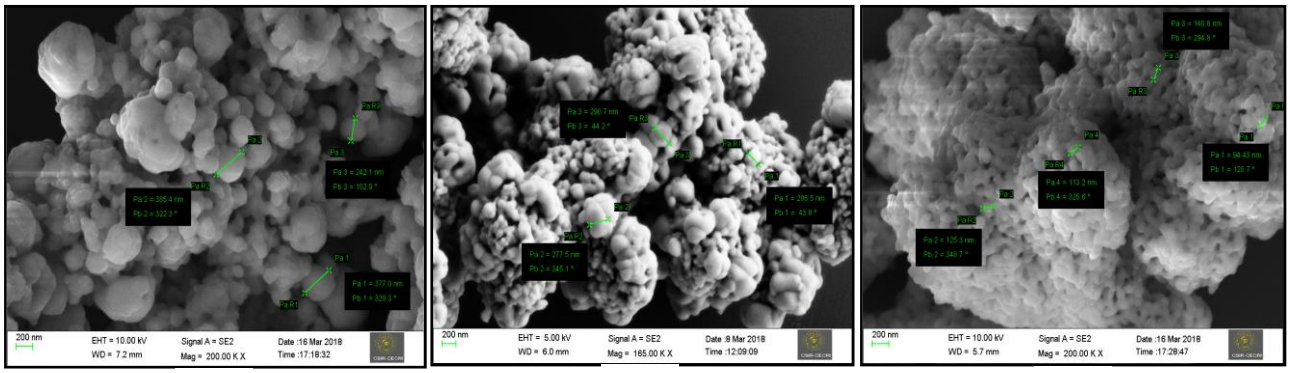

**(a)** **(b)** **(c)**

Fig.3.FESEM images of Mg- BTO at various concentrations (a) 0.25M (b) 0.50M (c) 0.75M

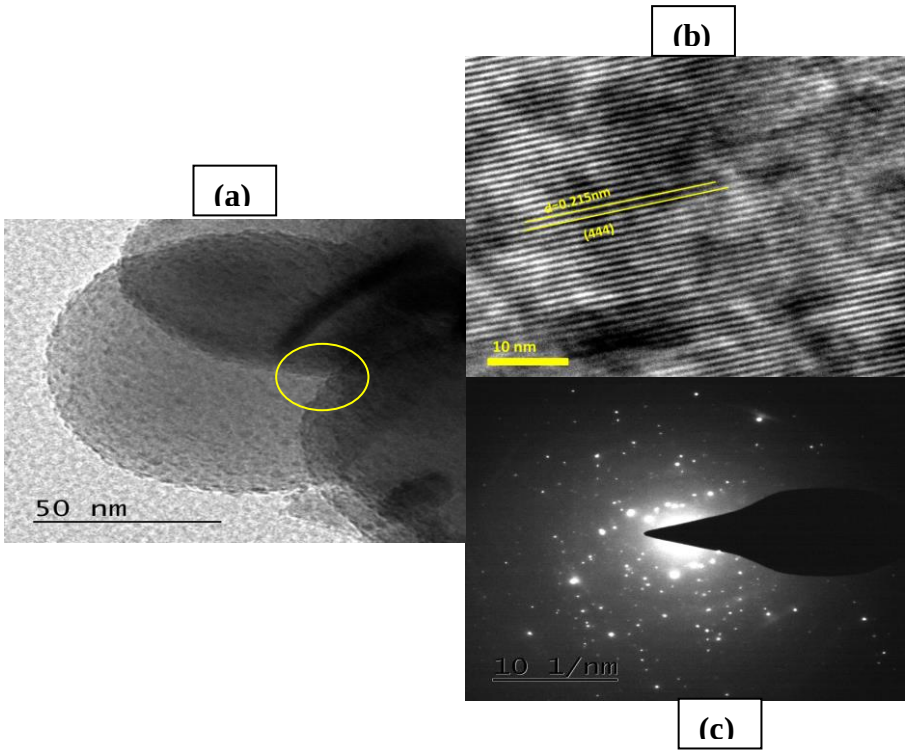


Fig.4. (a) HRTEM image of Mg-BTO (b) Enlarged view of fig.4a (c) SAED pattern of Mg-BTO

Table.1. Color coordinates measurement of magnesium doped bismuth titanate

| Sample | Color Coordinates | | |
|---|---|---|---|
| | L* | a* | b* |
| 0.25M | 96.72 | -6.34 | 13.11 |
| 0.50M | 97.28 | -6.70 | 14.25 |
| 0.75M | 97.47 | -6.30 | 15.85 |

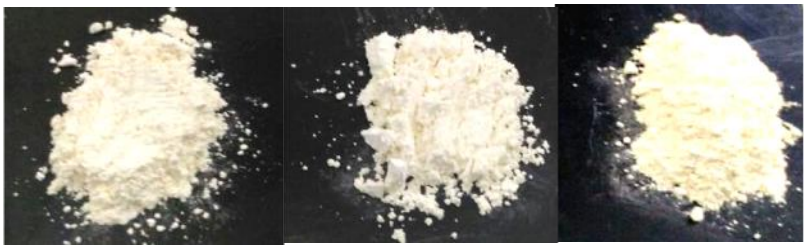

**(a)** **(b)** **(c)**

Fig.5. Photograph of magnesium doped bismuth titanate (a) 0.25M (b) 0.50M (c) 0.75M

***3.7. NIR diffuse reflectance Studies:***

The IR reflectance graph of Mg-BTO is shown in fig.6a.The reflectance of the pigment doped with various concentrations (0.25M, 0.50M, and 0.75M) of magnesium was compared. By increasing the dopant concentration upto 0.50M, the reflectance value gets increases slightly. The reflectance value gets decreases to a negligible value at a dopant concentration of 0.75M. The increase in reflectance is due to the decrease in the particle size. The reflectance can be affected by various factors like particle size, particle size distribution, packing density, etc. According to Kubelka-Munk Theory, the particle size and the scattering coefficient are inversely proportional. Scattering coefficient increases and the reflectance increases by decreasing the particle size. Due to this reason the reflectance get increases by decreasing the particle size. The results show that the Mg-BTO possess IR reflectance of 99.5% - 99.7% for various concentrations of magnesium. The IR reflectance property of undoped BTO and Mg-BTO is compared in fig.6b. The Mg-BTO shows higher IR reflectance property than undoped BTO. The IR solar reflectance spectra were determined with ASTM standard G173-03 [31]. The IR solar reflectance values of Mg-BTO are 98.92%, 100.21% and 99.90% for various concentrations of 0.25M, 0.50M and 0.75M. The IR solar reflectance graph was shown in fig.6c.

**3.8.** ***Chemical and Thermal stability of the Pigment:***

The chemical stability of the Mg-BTO pigment was tested in 10% solution of $H_2SO_4$, $HNO_3$, NaOH, HCl and $H_2O$. The pre-weighed Mg-BTO was allowed to stir in the acid/alkali/water solution for about 2 h. The treated pigment was allowed for washing in distilled water until the pH becomes neutral. Then the pigment is allowed to dry. Negligible weight loss is noticed for all samples. The color coordinates was measured for the chemically treated sample and the same was compared with the untreated sample. The color coordinates values are tabulated in Table.2. only negligible variation was noticed in color coordinates values on comparison with the untreated sample. The total color difference $\Delta E^*_{ab}$ values are tabulated in table.2. The acceptable limits of color difference are: $\Delta E^*_{ab} \leq 1$ unit (indistinguishable color change) whereas $\Delta E^*_{ab} \leq 5$ units is considered as very good.

Table.2: CIE $\Delta E^*_{ab}$ color differences of BTO nano pigment after acid/alkali/water resistance test

| Sample | Color coordinates | | | $\Delta E^*_{ab}$ |
|---|---|---|---|---|
| | L* | a* | b* | |
| $H_2O$ treated | 96.76 | -6.45 | 14.16 | 0.55 |
| $H_2SO_4$ treated | 96.01 | -6.28 | 14.05 | 1.19 |
| $HNO_3$ treated | 96.17 | -6.19 | 14.02 | 0.75 |
| NaOH treated | 96.65 | -6.25 | 14.23 | 0.61 |
| HCl treated | 96.24 | -6.15 | 14.06 | 0.97 |

$$\Delta E^*_{ab} = [(\Delta L^*)^2+(\Delta a^*)^2+(\Delta b^*)^2]^{1/2}$$

The thermal stability of Mg-BTO is confirmed from the TGA thermogram in a temperature range from 0 to 1200 ºC in a nitrogen atmosphere and shown in figure.7. The thermogram of undoped BTO and Mg-BTO was compared in fig.7. The thermogram of Mg-BTO shows a gradual weight loss with a residual mass of 91.16% while for undoped BTO the residual mass is 72.48% at 1200ºC. This shows that the Mg-BTO has good thermal stability than undoped BTO due to high bond dissociation energies of Mg-O bond (360kJ/mol) than the weak Bi-O bond dissociation energy (330kJ/mol). Mg-BTO shows 8.84% weight loss which is may be due to loss of moisture and some moieties like $Bi_2O_3$.

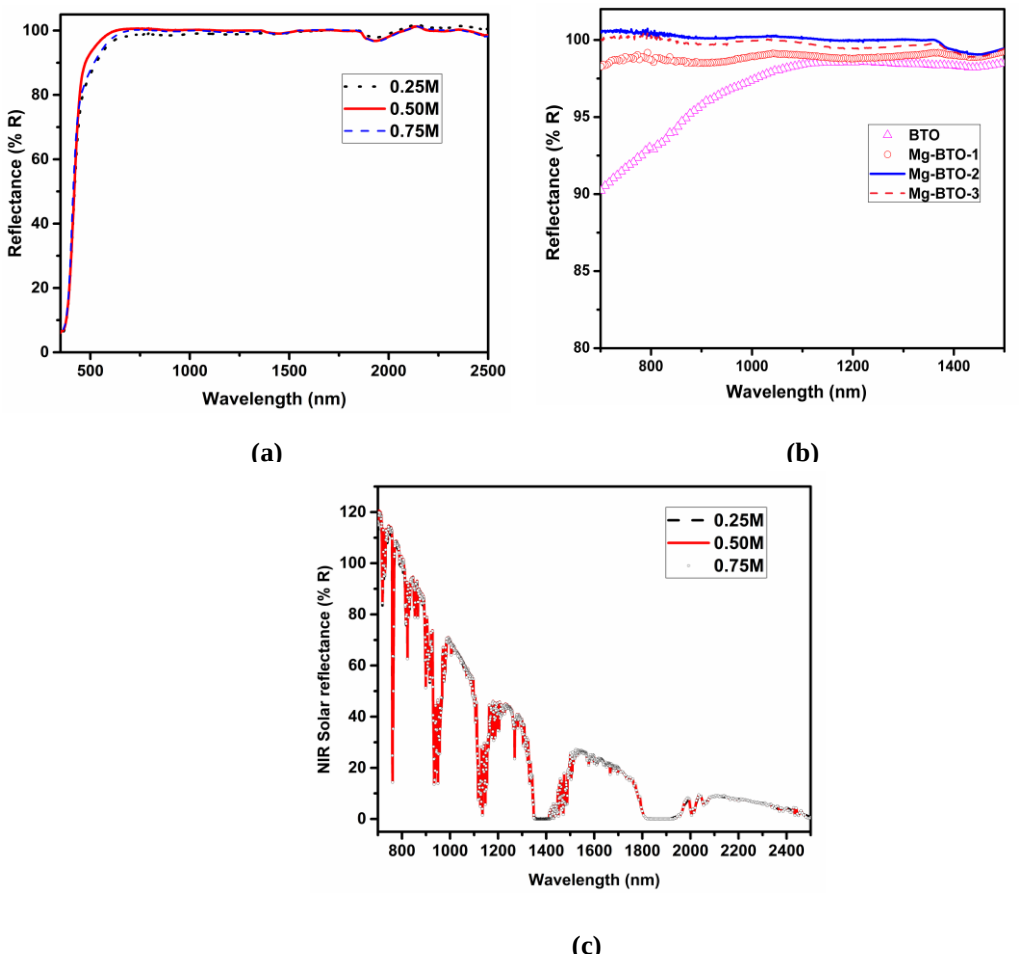


Fig.6. (a) IR reflectance graph of Mg-BTO (b) Comparison of IR reflectance of BTO and Mg-BTO (c) IR solar reflectance spectrum of Mg-BTO.

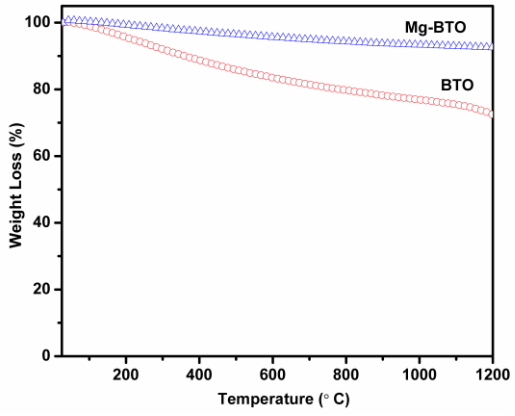


Fig.7. Thermogram of undoped BTO and magnesium doped BTO

### *3.9. Temperature study*

The IR reflective paint coated mild steel plates were allowed to expose in front of the infrared lamp as explained in [1]. Experimental setup of the temperature study is shown in fig.8a. As described in [1], the painted plates were kept 30 cm away from the infrared lamp and two thermocouples were used to record the temperature of the steel substrate, while one in front and the other at the back side of the plate. The plates were allowed under IR lamp for the period of 8 h. The time required to equilibrate the temperature is 1 h. After the equilibration time period, the temperature of the plate was recorded. The difference between the temperature in front (coated) and in the back (uncoated) side of the steel plates was recorded for the indication of IR reflective performance of the pigment. The results of temperature differences of the coatings were tabulated in table.3.

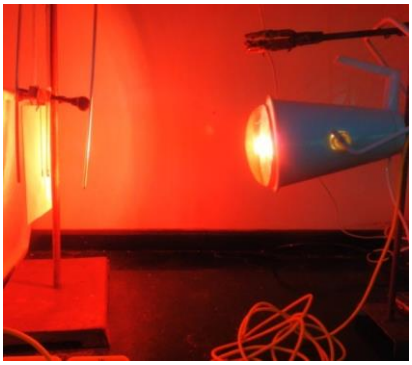

Fig 8a. Experimental setup for measuring temperature on coated steel substrates under IR lamp exposure

## 4. CONCLUSION

An infrared reflective Mg-BTO pigment with high IR reflectance (R = 99%) was synthesized using simple hydrothermal method. The IR reflectance property of Mg-BTO was measured using UV-Vis-NIR spectrophotometer and the potential application of Mg-BTO pigment as "cool pigment" was found by the thermal study using the IR lamp exposure. The thermal study showed that Mg-BTO coated steel substrate reduces the interior temperature by almost 9.7ºC which confirms the application of Mg-BTO as "cool pigment". The above results conclude that the Mg-BTO pigment will be a potential "cool pigment" with high NIR reflectance property and cheaper in cost for energy saving application.

Table 3. Temperature in front and behind the painted plates

| S.NO | SAMPLE | THICKNESS OF COATING (µm) | TEMPERATURE IN FRONT OF PANEL (ºC) | TEMPERATURE IN BEHIND THE PANEL (ºC) | TEMPERATURE DIFFERENCE (ºC) |
|---|---|---|---|---|---|
| 1. | Mg-BTO coated steel substrate | 153 | 42.6 | 32.9 | 9.7 |

The thermal image of Mg-BTO IR reflective paint coated glass substrate is shown in Fig.8b. The thermal image captured from FLIR C2 thermal Imaging camera shows a temperature difference of 9.6ºC (Mg-BTO). These results also confirm the IR reflective application of Mg-BTO.

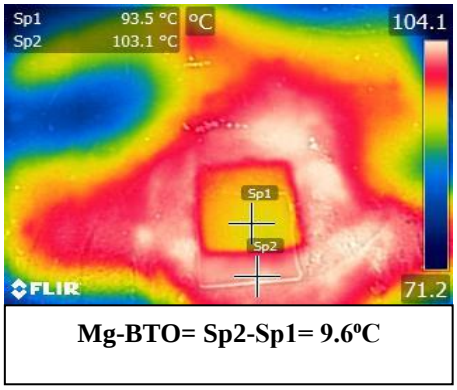


Fig.8b. Thermal Image of Mg-BTO paint coated glass substrate. Sp1= Temperature of glass substrate with coating; Sp2= Temperature of glass substrate without coating.

**Acknowledgements:**

The authors acknowledge Director of CSIR-CECRI for his moral support on this work.

**REFERENCES:**

[1]. Eliane Coser, Vicente Froes Moritz, Arno Krenzinger, Arthur Ferreira. (2015): Development of paints with infrared radiation reflective properties, Polímeros, 25, pp.305-310.

[2]. Libbra, A., Tarozzi, L., Muscio, A., & Corticelli, M. A. (2011): Spectral response data for development of cool coloured tile coverings, Optics & Laser Technology, 4, pp.394-400.

[3]. Ashwini K. Bendiganavale and Vinod C. Malshe, A. (2008): Infrared Reflective Inorganic Pigments, Recent Patents on Chemical Engineering, 1, pp. 67-79.

[4]. Levinson, R., Berdahl, P., Akbari, H. (2005): Solar spectral optical properties of pigments—Part I: model for deriving scattering and absorption coefficients from transmittance and reflectance measurements, Solar Energy Materials and Solar Cells, 89, pp.319-349.

[5]. Kaur, B., Quazi, N., Ivanov, I., & Bhattacharya, S. N. (2012): Near-infrared reflective properties of perylene derivatives, Dyes and Pigments, 92, pp.1108-1113.

(1)

[6]. Jungang Hou, Shuqiang Jiao, Hongmin Zhu, R.V.Kumar. (2011): Bismuth titanate pyrochlore microspheres: Directed Synthesis and their visible light photocatalytic activity, Journal of Solid State Chemistry, 184, pp.154-158.

[7]. J. Roberto Esquivel-Elizondo, Beverly Brooks Hinojosa, and Juan C. Nino. (2011): $Bi_2Ti_2O_7$: It Is Not What You Have Read, Chemistry of Materials, 23, pp. 4965–4974.

[8].Subramanian, M.A., Aravamudan, G., and Subba Rao, G.V. (1983) : Oxide Pyrochlores- A Review, Progress in Solid State Chemistry, 15, pp. 55-143.

[9]. R.D.Shannon. (1976): Revised Effective Ionic Radii and Systematic Studies of Interatomic Distances in Halides and Chaleogenides, Acta Crystallographic a, 32, pp.751-767.

[10]. D. P. Cann, C. A. Randall, and T. R. Shrout. (1996) : Investigation of the Dielectric Properties of Bismuth Pyrochlores, Solid State Communication, 100, pp. 529–534.

[11]. J. C. Nino, M. T. Lanagan, and C. A. Randall, (2001) : Dielectric Relaxation in $Bi_2O_3$-ZnO-$Nb_2O_5$ Cubic Pyrochlore, Journal of Applied Physics, 89, pp.4512–4516.

[12]. S. Kamba, V. Porokhonskyy, A. Pashkin, V. Bovtun, J. Petzelt, J. C. Nino, S. Trolier-McKinstry, M. T. Lanagan, and C. A. Randall. (2002) : Anomalous Broad Dielectric Relaxation in Bi1.5Zn1.0Nb1.5O7 Pyrochlore, Physical Review B, 66, pp.054-106.

[13]. J. Banys, M. Ivanov, S. Rudys, J. Li, and H. Wang. (2010): Dielectric Properties of Cubic Bismuth Based Pyrochlores Containing Lithium and Fluorine, Journal of the European Ceramic Society, 30, pp.385–388.

[14]. H. L. Du, X. Yao, and H. Wang. (2008) : Relaxor-Like Behaviour of Bismuth Based Pyrochlores Containing Sn, Journal of Electro ceramics, 21, pp.222–225.

[15]. Y. Liu, R. L. Withers, H. B. Nguyen, K. Elliott, Q. Ren, and Z. Chen. (2009) : Displacive Disorder and Dielectric Relaxation in the Stoichiometric Bismuth-Containing Pyrochlores, $Bi2M^{III}NbO_7$ (M=In and Sc), Journal of Solid State Chemistry, 182, pp.2748–2755.

[16]. M. Valant. (2009) : Dielectric Relaxations in Bi2O3–Nb2O5–NiO Cubic Pyrochlores, Journal of the American Ceramic Society, 92, pp. 955–958.

[17]. Oliver Merka, Detlef W. Bahnemann, Michael Wark. (2014) : Photocatalytic hydrogen production with non-stoichiometric pyrochlore bismuth titanate, Catalysis Today, 225,pp. 102–110.

[18]. Sankaran Murugesan, Muhammad N. Huda, Yanfa Yan, Mowafak M. Al-Jassim, and Vaidyanathan (Ravi) Subramanian. (2010) : Band-Engineered Bismuth Titanate Pyrochlores for Visible Light Photocatalysis, Journal of Physical Chemistry C, 114, pp.10598–10605.

[19]. Wei F. Yao, Hong Wang , Xiao H. Xu , Jing T. Zhou , Xue N. Yang , Yin Zhang , Shu X. Shang. (2004) : Photocatalytic property of bismuth titanate $Bi_2Ti_2O_7$, Applied Catalysis A: General, 259, pp. 29–33.

[20]. Hongjun Zhou, Tae-Jin Park and Stanislaus S. Wong. (2006) : Synthesis, characterization, and photocatalytic properties of pyrochlore $Bi_2Ti_2O_7$ nanotubes, Journal of Materials Research, 21, pp.2941-2947.

[21] Levinson, R.; Berdahl, P.; Akbari, H. (2005): Solar spectral optical properties of pigments-Part II: Survey of common colorants. Solar Energy Materials and Solar Cells. 89, pp.351−389.

[22] Rui Yang, Aijun Han, Mingquan Ye, Xinging Chen, Lin Yuan. (2017): Synthesis, Characterization and thermal performance of Fe/N co-doped $MgTiO_3$ as a novel high near-infrared reflective pigment. Solar Energy Materials and Solar Cells, 160, pp.307-318.

[23]. Paraman Meenakshi, Muthiah Selvaraj. (2018): Bismuth titanate as an infrared reflective pigment for cool roof coating, Solar Energy Materials and Solar Cells, 174, pp.530-537.

[24]. Robert lanos, Eliza Muntean, Roxana Babuta, Radu Lazau, Cornelia Pacurariu, Cornelia Bandas. (2017): Combustion synthesis of pink chromium-doped alumina with excellent near-infrared reflective properties. Ceramics International, 43, pp. 2568-2572.

[25]. Rui Yang, Aijun Han, Mingquan Ye, Xingxing Chen, Lin Yuan. (2017): The influence of Mn/N co-doping on the thermal performance of ZnAl2O4 as high near-infrared reflective inorganic pigment. Journal of Alloys and Compounds, 696, pp.1329-1341.

[26]. Estibaliz Aranzabe, Pedro Maria villas ante, Ricard March, Maria Isabel Arriortua, Julen Vadillo, Aitor Larrang, Ana Aranzabe. (2016): Preparation and characterization of high NIR reflective pigments based in Ultramarine blue. Energy and Buildings, 126, pp.170-176.

[27]. A.G.Krasnov, I.V.Piir, M.S.Koroleva, N.A.Sekushin, Y.I.Ryabkov, M.M.Piskaykina, V.A.Sadykov, E.M.Sadovskaya, V.V.Pelipenko, N.F.Eremeev. (2016): The conductivity and ionic transport of doped bismuth titanate pyrochlore $Bi_{1.6}M_xTi_2O_{7-\delta}$ (M – Mg, Sc, Cu), Solid State Ionics, 302, pp.118-125.

[28] A. G. Krasnov, M. M. Piskaikina, and I. V. Piir. (2016) : Synthesis and Properties of Sc- and Mg-Doped Bismuth Titanates with the Pyrochlore Structure, Russian Journal of General Chemistry, 86, pp.205–212

[29] Kun Qian , Li Xia , Wei Wei , Linlin Chen , Zhifeng Jiang , Junjie Jing , Jimin Xie. (2017): Construction of $Bi_2Ti_2O_7/Bi_4Ti_3O_{12}$ composites with enhanced visible light photocatalytic activity, Materials Letters, 206, pp. 245–248.

[30]. Sankaran Murugesan and Vaidyanathan (Ravi) Subramanian. (2009): Robust synthesis of bismuth titanate pyrochlore nanorods and their photocatalytic applications, Chemical Communications, 34, pp.5109–5111.

[31] Standard tables for reference solar irradiance: Direct normal and hemispherical on 37 tilted surface. ASTM International. West Conshohocken, PA 2012.